Isolating the Contributions from Moments of Inertia in Isotopic Shifts Measured by High-Resolution Cyclic Ion Mobility Separations

David L. Williamson, Haisley M. Windsor, Gabe Nagy *

Department of Chemistry, University of Utah, 315 South 1400 East, Room 2020, Salt Lake City, Utah 84112, United States

Corresponding author: gabe.nagy@utah.edu

Abstract

The unexpected finding that isotopomers (i.e., isotopic isomers) can be separated with high-resolution ion mobility spectrometry-mass spectrometry (IMS-MS) has raised new structural considerations affecting an ion's mobility—namely, its center of mass (CoM) and moments of inertia (MoI). Unfortunately, thus far, no studies have attempted to experimentally isolate either CoM or Mol, as they are intrinsically linked by their definitions, where Mol is calculated in relation to CoM. In this study, we designed and synthesized four isotopically labeled tetrapropylammonium (TAA3) ions, each with unique mass distributions. Three of the synthesized TAA3 ions were labeled symmetrically, thus having identical CoM but differing MoI, which we verified using density functional theory (DFT) calculations. Consequently, we were able to isolate the effect of MoI changes in high-resolution IMS-MS separations. Cyclic ion mobility spectrometrymass spectrometry (cIMS-MS) separations of the isotopically labeled TAA3 variants revealed isotopic mobility shifts attributable solely to changes in Mol. A 60-meter cIMS-MS separation demonstrated that two nominally isobaric TAA3 pseudoisotopomers could be partially resolved, showcasing potential feasibility for isotopomer separations on commercially available IMS-MS platforms. With our previously established collision cross section (CCS) calibration protocol, we also quantified the relationship between Mol and CCS. Our results represent the first demonstration of IMS-MS separations based solely on MoI differences. We believe these findings will contribute important evidence to the growing body of literature on the physical nature of isotopic shifts in IMS-MS separations and work toward more accurate CCS predictions.

Introduction

lon mobility spectrometry coupled to mass spectrometry (IMS-MS) is an analytical technique where ions are separated in the gas phase under the influence of an electric field by their size, shape, and charge (i.e., their ion mobilities).^{1, 2} In recent years, the development of traveling-wave based IMS-MS platforms (e.g., structures for lossless ion manipulations, SLIM and cyclic IMS, cIMS) has enabled much longer pathlength separations to be possible, and thus has enabled tremendous increases in achievable resolution.³⁻⁸ These high-resolution IMS-MS separations have enabled advances in omics-based analyses specifically as related to isomers with subtle structural differences often on the order of <1% differences in their rotationally-averaged ion neutral collision cross sections (CCS).⁹⁻¹³

More recently, high-resolution IMS-MS platforms have begun to study the effects of mass distribution (i.e., changes in center of mass, CoM, and moments of inertia, MoI) in the separations of isotopologues and isotopomers. 14-24 Previous work focused on naturally-occurring isotopologues (e.g., 13C, 37Cl, and 81Br) as well as molecules that were derivatized with stable heavy isotopes. 14-24 It has been demonstrated that these mass distribution-based isotopic shifts can be isomer and conformer specific in nature as well as orthogonal to CCS thus potentially providing analytical utility through a two-dimensional approach for unknown characterization. 25-27 Additionally, computational work has demonstrated good agreement between simulated rotational effects in IMS-MS and experimental results of mass distribution-based isotopic shifts. 28, 29

However, while it has been established that mass distribution is the cause of these observed isotopic shifts, a more comprehensive understanding of the roles that both center of mass (CoM) and moments of inertia (MoI) play has been difficult to deconvolute. The primary obstacle is the intrinsic relationship between CoM and MoI, where MoI is calculated in relation to CoM. To overcome this, we designed and synthesized a system of isotopomers to have perfectly symmetrical isotopic labeling in their ionized form, resulting in sets of isotopomers that have the

same CoM but different MoI, thus allowing us to experimentally isolate the effect of MoI with high-resolution cIMS-MS separations.

Experimental Section

Reagents, Conditions, and cIMS-MS Parameters.

Tetrapropylammonium (TAA3), ammonia and ammonia-15N solutions (both in methanol), and 1-Bromopropane-2,3-13C₂ were purchased from Sigma-Aldrich (Milwaukee, WI, USA). All deuterated forms of 1-Bromopropane were purchased from CDN Isotopes (Quebec, Canada). LC-MS grade solvents were purchased from Fischer Scientific (Pittsburg, PA, USA). Stock solutions for TAA3 and its isotopologues/isotopomers were prepared in 100% methanol. Each analyzed sample was diluted to a final concentration falling between 1 and 5 μ M in 49.75/49.75/0.5 (v/v) water/methanol/acetic acid. Final concentrations for each isomer varied to ensure that the total signal intensity was approximately 1e4 to reduce detector saturation and potential unwanted space-charge effects. The Waters cyclic ion mobility spectrometry-mass spectrometry (cIMS-MS) system (Wilmslow, UK) used in these experiments is commercially available and has been described in previous publications.^{3, 30} Briefly, each sample was subjected to positive ion mode electrospray ionization (2.5 kV) with a flow rate of 2 μL/min. A quadrupole isolate the desired m/z range, which encompassed the desired was used to isotopologues/isotopomers of interest in each respective separation. Ions were separated around the 1 m cIMS separation region by pulsed DC traveling waves in nitrogen buffer gas at a pressure of 1.74 mbar. The cIMS array allows ions to be cycled multiple times around the separation region, increasing the IMS resolution and resolving power. After the cIMS separation, ions were ejected to the TOF-MS, operated in V-mode, for detection. All arrival time distribution data was m/z extracted using our TOF-MS.

Synthesis of TAA3 Isotopologues and Isotopomers

To synthesize the TAA3 isotopomers, the general procedure for the direct alkylation of ammonia was followed. 31,32 0.2g (1.6 mmol) of 1-Bromopropane-1,1-d₂, 1-Bromopropane-2,2-d₂, or 1-Bromopropane-2,3- 13 C₂ respectively was added to 20 μ L of 2.0 M ammonia in methanol within a microcentrifuge tube (see Figure S1 for reaction schematic). The sample was then diluted with methanol to a final volume of 500 μ L and heated at 50 °C in a sealed tube for 24 hours. After subsequent heating, any evaporated methanol was replaced to give a final volume of 500 μ L. For the asymmetrically labeled TAA3- 15 Nd₇, a 3:1 ratio of unlabeled 1-Bromopropane-d₇ was reacted with 15 NH₃ to produce labeling on a single leg. Each synthetically produced, labeled isotopomer was then diluted to give similar intensities as the unlabeled TAA3 isotopologue. We note that any potential side products are non-isobaric to our product of interest and thus can be differentiated by m/z.

Data Processing and CCS Calculations

Data was acquired using MassLynx and Quartz. Signal averaging was performed for 3 minutes for all 20-meter data and 2 minutes for the calibrants used in CCS calibration. For the 60-meter separation of the mixture of $(1,1-d_2)_4$ -TAA3 isotopomer and $2,3-^{13}C_2$ -TAA3, 10-minutes of signal averaging was used with a subsequent 10-point Savitsky-Golay smooth to produce the arrival time distribution. All other arrival time distributions shown were constructed by using raw signal averaged data with no additional smoothing or data processing. Origin 2020 was used to generate a best-fit Gaussian distribution which calculated the peak apexes (i.e., arrival times). We would like to emphasize that the Gaussian fitting to determine arrival times was always performed on the raw, unsmoothed data. Relative arrival time values $(t_{Rel.})$ values were determined using Equation 1 where t_{heavy} and t_{light} refer to the arrival times of the heavy and light isotopologues. Relative arrival times were averaged across three trials on three different days for

all compounds. It is important to note that the use of $t_{Rel.}$ based analysis is suitable for isotopologues/isotopomers present within a mixture, as demonstrated in previous publications, and results in higher precision than what is possible from individual absolute arrival times.^{25-27, 29}

$$t_{Rel.}(\%) = \left(\frac{t_{heavy}}{t_{light}} - 1\right) \times 100 \tag{1}$$

CCS values were calculated with our previously established method involving the use of average ion velocity. ³³ Specifically, a calibration curve was produced by three independent trails of unlabeled tetraethylammonium (TAA2), TAA3, and tetrabutylammonium (TAA4) at a pathlength of 4 m (see Supporting Information Figure S2). Arrival times were adjusted to account for the time ions spent outside of the cyclic mobility region (i.e., t₀/dead time); this calculation has been explained in previous publications. ^{34,35} The apex of the arrival time peaks for each unlabeled TAA and CCS values were converted into average ion velocities and reduced CCS values, respectively. To calculate the CCS values for the TAA3 isotopologues and isotopomers, we first averaged the arrival times for the unlabeled (d₀) to generate an average t_{light} value across all 12 trials. From there, we used the experimental t_{Rel.} values and the average t_{light} value to generate average t_{heavy} values and their corresponding errors from triplicate trials for the TAA3 isotopologues and isotopomers. These t_{heavy} values were converted into average ion velocities, then CCS values through our calibration curve. For a detailed workflow and example calculation for converting t_{Rel.} values into CCS values and their respective errors, please see Figures S3 and Table S2 in the Supporting Information.

Computational Details

The structures of all TAA3 compounds were modeled using density functional theory (DFT). Each structure was calculated at the B3LYP level of theory with basis set 6-311G ++ using

the Gaussian 16 software package.³⁶ This level of theory has been previously used for DFT optimized structures of ammonium salts in the gas phase.³⁷ Mol values were pulled directly from Gaussian 16 outputs, where they are calculated as part of the vibrational analysis.³⁸ CoM calculations were performed using the DFT optimized xyz coordinates and atomic masses. For the gas phase structure and xyz coordinates, please see Figures S4 and Table S4 in the Supporting Information. Our CoM calculations assume that the atomic positions of the isotopomers are identical. It should be noted that minor shifts in the atomic positions could be possible based on the isotope effect. However, any shifts in CoM resulting from this would be negligible in magnitude and are thus not accounted for in these experiments.

Results and Discussion

Synthesis of TAA3 Isotopomers

Our simple, one step, reaction to generate isotopomers uses isotopically labeled alkyl halides (i.e., 1-Bromopropane-1,1-d₂). Therefore, our synthesized products relied on which alkyl halides were commercially available. We found that the TAA3 system would offer the greatest flexibility in the number of isotopomers and pseudoisotopomers that could be generated, where isotopic labels are on different atoms such as ¹³C versus ²H (d). From the available isotopically labeled reagents, there were no other possible isotopomers or pseudoisotopomers that could be synthesized using direct alkylation other than the ones presented in this work. We initially tested our methodology by performing the reaction of unlabeled 2-bromopropane with NH₃ where we observed the expected [M]* peak of TAA3 at *m*/*z* 186.22. After validating our procedure, we repeated it with two deuterated versions of 1-Bromopropane (1-Bromopropane-1,1-d₂ and 1-Bromopropane-2,2-d₂) to generate two TAA-d₈ isotopomers (see Figure 1). In addition to the two isotopomers, we also generated two pseudoisotopomers, one with a ¹³C labeled version of 1-Bromopropane (1-Bromopropane-2,3-¹³C₂), and another with a mixture of fully deuterated 1-

Bromopropane-d₇ and unlabeled 1-Bromopropane reacted with ¹⁵NH₃ to give a TAA3-¹⁵Nd₇ pseudoisotopomer (see Supporting Information, Figure S2).

$$NH_{3} + \bigcup_{D \in D} Br$$

$$excess$$

$$NH_{3} + \bigcup_{D \in D} Br$$

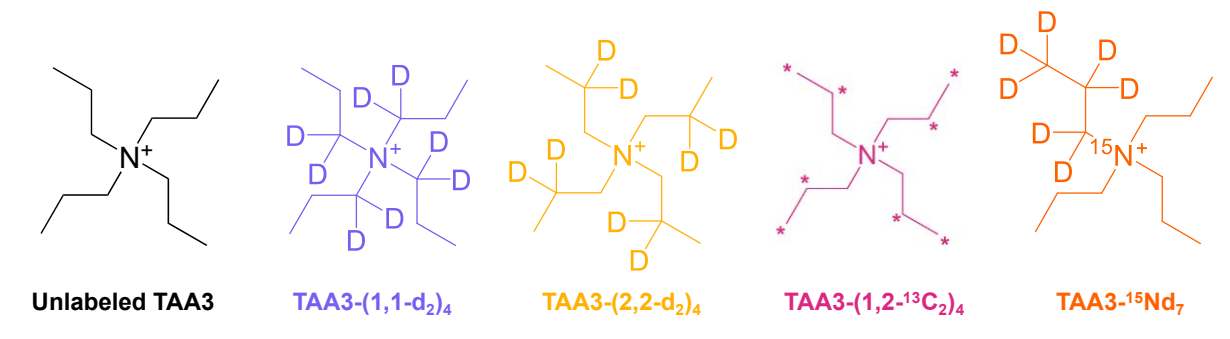
$$excess$$

Figure 1. Synthesis scheme and structures of TAA3-(1,1-d₂)₄ and TAA3-(2,2-d₂)₄ isotopomers.

Structures, Mol, and CoM Calculations for TAA3 Isotopomers

After synthesizing the desired isotopomers and pseudoisotopomers according to the procedure outlined in the Experimental Section, we performed computational analyses. We began with two goals in mind: 1) verify that the three symmetrically labeled configurations, TAA3-(1,1-d₂)₄, TAA3-(2,2-d₂)₄, and TAA3-(¹³C₂)₄, had identical CoM and 2) quantify the differences in Mol between the various structures relative to the unlabeled TAA3 isotopologue. We found that the CoM stayed at the center of the molecule (i.e., at the coordinates of the nitrogen) for all species except TAA3-¹⁵Nd₇, which exhibited a CoM shift approximately 1% of the molecule length, as expected from the asymmetric labeling. The Mol for each isotopomer and pseudoisotopomer was also calculated as part of the vibrational analysis and given in the output file of the structure calculation.³⁸ Changes in Mol can be observed in one or more of the I_{xx}, I_{yy}, and I_{zz} axis. Therefore, to directly compare changes in Mol between isotopomers, the three values were summed then

divided by the unlabeled TAA3 isotopologue, giving summed relative inertia values (relative $\Sigma_{inertia}$) as displayed in Figure 2.



		Center of Mass			Moment of Inertia
Species	m/z	X (Å)	Y (Å)	Z (Å)	Relative Σ _{inertia}
Unlabeled TAA3	186.22	0.00	0.00	0.00	1.000
TAA3-(1,1-d ₂) ₄	194.27	0.00	0.00	0.00	1.024
TAA3-(2,2-d ₂) ₄	194.27	0.00	0.00	0.00	1.044
TAA3-(1,2-13C ₂) ₄	194.25	0.00	0.00	0.00	1.059
TAA3-15Nd ₇	194.26	-0.07	-0.08	0.00	1.054

Figure 2. Structures and CoM/Mol values for TAA3 isotopomers and pseudoisotopomers.

cIMS-MS Separations of TAA3 Isotopomers and Pseudoisotopomers

After synthesizing the isotopically labeled variants of TAA3 (i.e., TAA3- $(1,1-d_2)_4$, TAA3- $(2,2-d_2)_4$, TAA3- $(1,2-^{13}C_2)_4$, and TAA3- $^{15}Nd_7$), we performed clMS-MS separations for each of them in a mixture with the unlabeled TAA3 isotopologue at a total pathlength of 20 meters (Figure 3). From these separations, we calculated the observed $t_{Rel.}$ values using Equation 1 and compared them amongst every synthesized isotopomer/pseudoisotopomer. From our clMS-MS separations and theoretical modeling calculations (Figure 2), we globally observed that increases in Mol introduced larger isotopic shifts (i.e., larger $t_{Rel.}$ values). For example, from Figure 3, the TAA3- $(1,1-d_2)_4$ isotopomer with a lower calculated change in Mol had a $t_{Rel.}$ value of 0.41% relative to the unlabeled TAA3 isotopologue, while the TAA3- $(2,2-d_2)_4$ isotopomer, with the larger magnitude change in Mol, had a larger observed $t_{Rel.}$ value of 0.67%. This was also evident when

analyzing the TAA3- $(1,2^{-13}C_2)_4$ isotopomer, which has the highest calculated MoI, and displayed a $t_{Rel.}$ value of 0.82%, which is approximately double that of the lowest calculated MoI, TAA3- $(1,1^{-1}d_2)_4$ species. For the asymmetric isotopomer (TAA3- $^{15}Nd_7$), it had a $t_{Rel.}$ value of 0.82%, identical to that of the TAA3- $(1,2^{-13}C_2)_4$ isotopomer, despite its considerable shift in CoM, approximately 1% of the molecule's length. This observation suggests that the cumulative effect of MoI and CoM on TAA3- $^{15}Nd_7$ shift is equivalent to that of MoI alone on TAA3- $(1,2^{-13}C_2)_4$.

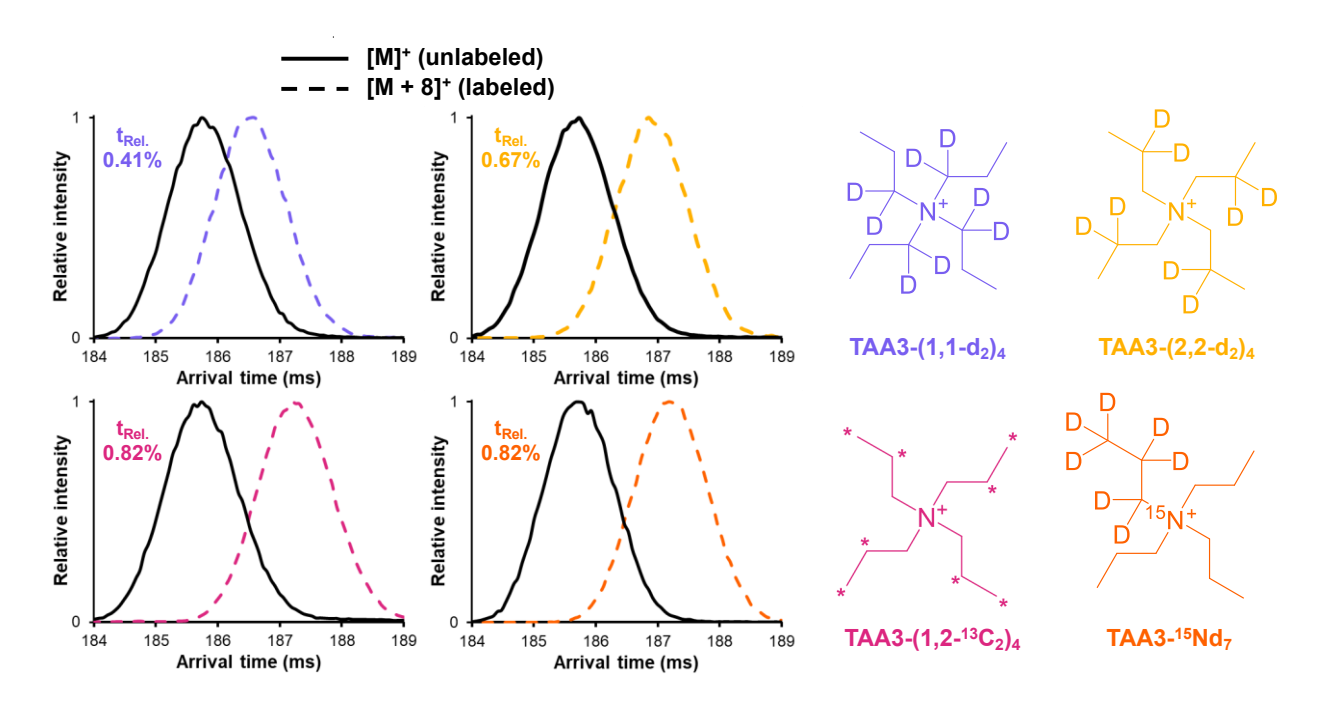


Figure 3. 20 m cIMS-MS separations of TAA3 isotopomers and pseudoisotopomers in a mixture with the unlabeled TAA3 isotopologue at traveling wave conditions of 650 m/s and 20 V.

Based on the observed differences in $t_{Rel.}$ values between TAA3-(1,1-d₂)₄ and TAA3-(1,2- $^{13}C_2$)₄ shown in Figure 3, we thought that it may be possible to resolve these two pseudoisotopomers at an extended clMS-MS separation pathlength. Additionally, since TAA3-(1,1-d₂)₄ and TAA3-(1,2- $^{13}C_2$)₄ are pseudoisotopomers (i.e., do not have identical m/z values; see Figure 2), they are resolvable in the m/z dimension. At a clMS-MS separation pathlength of 60 meters (Figure 4), we observed that these two pseudoisotopomers (i.e., TAA3-(1,1-d₂)₄ and

TAA3-(1,2-¹³C₂)₄) could indeed be resolved based on their respective differences in moments of inertia. Interestingly, this echoes our previous results with 4-iodoaniline where we observed an inverse arrival time order for deuterated isotopologues (i.e., where the heavier isotopologue arrives before the lighter one).²⁶ In this instance, the mass difference is marginal, with TAA3-(1,1-d₂)₄ being approximately 23 mDa heavier than TAA3-(1,2-¹³C₂)₄. However, this still presents a notable example where the mass distribution-based shift stemming from changes in moments of inertia can overcome reduced mass contributions.

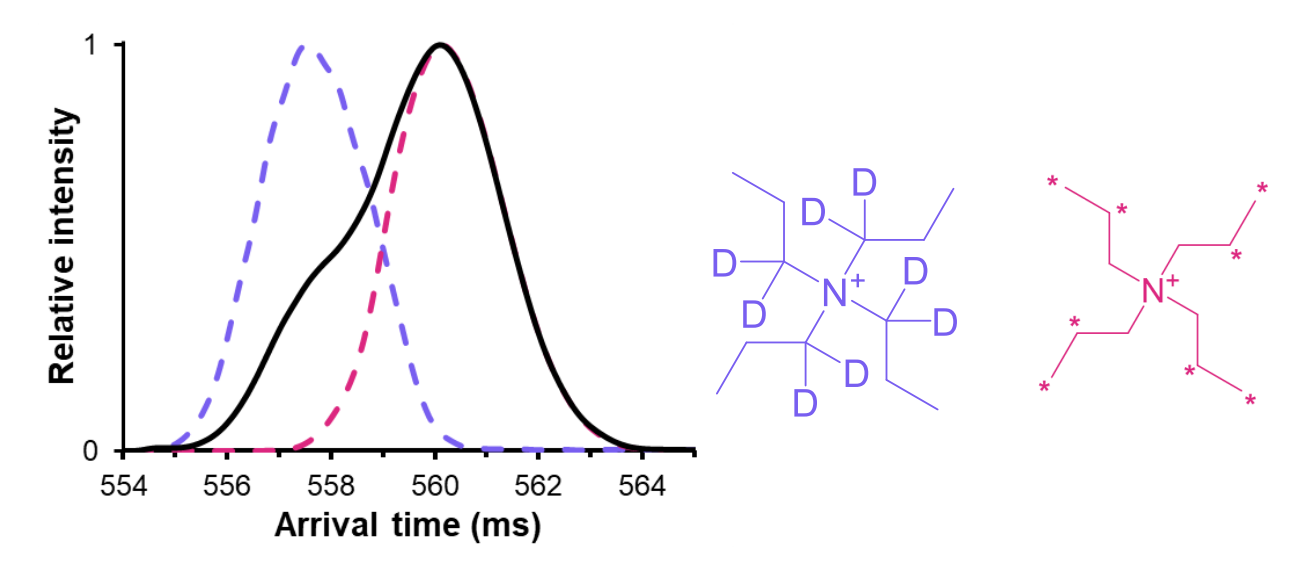


Figure 4. 60-meter cIMS-MS separation of the TAA3- $(1,1-d_2)_4$ (m/z 194.27) and TAA3- $(1,2^{-13}C_2)_4$ (m/z 194.25) isotopomers as their [M]⁺ at the same traveling wave conditions in Figure 3. The black trace represents the mixture, while the dashed traces are the overlaid individual species. Differences in intensity are attributed to varying reaction yields.

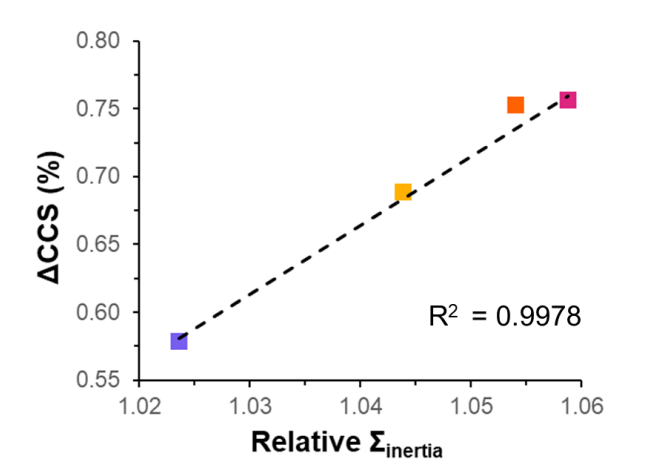
Correlating Moments of Inertia and Collision Cross Section Values

From our theoretical calculations of changes in moments of inertia from Figure 2, the cIMS-MS separations, and corresponding $t_{Rel.}$ values in Figure 3, we qualitatively observed that increases in moments of inertia resulted in greater $t_{Rel.}$ values (i.e., larger changes in MoI resulted in higher resolution of the labeled TAA3 isotopomers from the unlabeled TAA3). However, we were interested in quantifying this relationship; specifically, we wanted to understand how our observed changes in MoI are reflected in differences amongst CCS values between

isotopomers/pseudoisotopomers. To do this, we used our previously established CCS calibration method involving the use of average ion velocities which enables CCS to be derived from ions subjected to varying cIMS-MS separation pathlengths (see Experimental Section and Supporting Information). We would like to mention that this work, along with our previous work in the area of isotopic shifts, have demonstrated ultrahigh precision in our calculated $t_{Rel.}$ values as compared to the precision that can be obtained from raw arrival times of an individual molecule. Additionally, others have recently reported SLIM-based separations which showed approximately an order of magnitude lower standard deviations in their reported Δ CCS values compared to that of raw CCS values. Thus, we envision that our calculated cIMS-MS-based CCS values also have high precision, but we do acknowledge that there may be some uncertainties in the absolute CCS based on the drift tube CCS calibrant values used.

Thus, instead of plotting raw CCS values, we chose to plot our calculated percent Δ CCS values for the TAA3 isotopomers and pseudoisotopomers relative to the unlabeled TAA3 isotopologue versus the relative moments of inertia values from Figure 2. In Figure 5, we observed a linear relationship with an R² value > 0.99 between our percent Δ CCS values and calculated changes in moments of inertia. While the theoretical relationship between MoI and CCS may not be linear (i.e., potentially reaching an asymptote), this system, and almost any other realistic system, of isotopomers are in a narrow enough mobility range and thus we would expect a linear relationship. As expected, the TAA3- 15 Nd $_7$ isotopomer falls off our linear trendline because of its changes in both center of mass and moments of inertia. Overall, Figure 5 highlights the good agreement between our experimental measurements (i.e., $t_{Rel.}$ values and percent Δ CCS) and the theoretical changes in moments of inertia introduced by isotopic labeling. From this data, we can estimate that the pseudoisotopomer separation shown in Figure 4 represents a Δ CCS value of \sim 0.18%. We attribute our observed relationship, where increases in MoI lead to increases in CCS for isotopomers, results from changes in rotational degrees of freedom, which dictates the transfer

of translational and rotational momentum. More specifically, higher Mol isotopomers result in collisions with greater transfer of translational to rotational momentum, resulting in lower mobilities. ²⁸



Species		Relative Σ _{inertia}	ΔCCS (%)	
TAA3-(1,	1-d ₂) ₄	1.024	0.579 ± 0.005	
TAA3-(2,	.2-d ₂) ₄	1.044	0.688 ± 0.008	
TAA3-(1,2	2- ¹³ C ₂) ₄	1.059	0.756 ± 0.009	
TAA3-1	⁵ Nd ₇	1.054	0.753 ± 0.009	

Figure 5. Correlation of theoretical MoI (Relative Σ_{inertia}) and Δ CCS for the TAA3 isotopomers and pseudoisotopomers.

Conclusions

While previous work in the area of isotopic shifts in high-resolution ion mobility separations has indicated that these shifts stem from changes in mass distribution, it was unclear whether contributions from center of mass and moments of inertia could be deconvoluted experimentally. To test this, we synthesized four isotopically labeled tetrapropylammonium (TAA3) ions, two of which were deuterated isotopomers, and two of which were pseudoisotopomers (i.e., including ¹³C and/or ¹⁵N atoms resulting in non-isobaric *m/z*). These syntheses yielded three species with identical center of mass as verified through DFT calculations. Our theoretical modeling revealed that the synthesized isotopomers differed in Mol by as much as 3%, with TAA3-(1,2-¹³C₂)₄ having the highest Mol and TAA3-(1,1-d₂)₄ having the lowest. We performed separations of each heavy labeled TAA3 isotopologue in a mixture with the unlabeled one, which allowed us to calculate

high precision t_{Rel.} values at a cIMS-MS separation pathlength of 20 meters. The measured t_{Rel.} values differed considerably, with TAA3-(1,2-13C₂)₄ having approximately two times the t_{Rel.} of TAA3-(1,1-d₂)₄, 0.82% vs 0.41%, respectively. To better quantify these Mol-based isotopic shifts, we used our previously developed CCS calibration approach to determine the percent differences in CCS for our synthesized isotopomers relative to the unlabeled TAA3 isotopologue. From this, we determined that a linear relationship existed between the relative changes in moments of inertia and the calculated cIMS-MS-based percent differences in CCS values for our TAA3 isotopomers and pseudoisotopomers, which we attribute to differing exchange between translational and rotational momentum. Based on these results, we also were able to perform a 60 m cIMS-MS separation and partially resolve two pseudoisotopomers that differ in their CCS values by ~0.18%. Overall, our findings are the first to demonstrate IMS-MS separations based solely on Mol differences. Our results broadly agree with previous computational experiments, which designed artificial isotopomers to predict the effects of MoI and CoM in isotopic shifts.²⁸ Those simulated isotopomer separations suggested that increases in Mol always lead to a higher CCS, while changes in CoM can result in an increase, decrease, or no change in CCS. ²⁸ We believe these results will be valuable for the IMS-MS community, enhancing our understanding of isotopic shifts in high-resolution IMS-MS separations and thus working toward more accurate CCS predictions. Our future work will involve developing similar systems of isotopomers and isotopologues to further deconvolute CoM and Mol contributions.

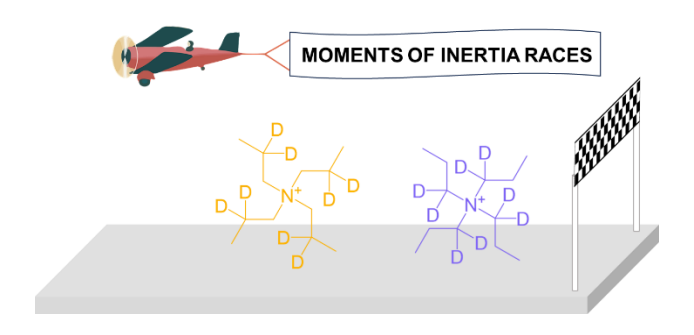
Supporting Information

Synthesis of isotopomers, CCS calibration curves, example CCS calculation, calculated moments of inertia, calculated centers of mass, DFT optimization.

Acknowledgments

We acknowledge the ACS Petroleum Research Fund (PRF) for the support of this work (ACS PRF 65998-DNI6). Additional support was provided by the NSF Research Experiences for Undergraduates (REU) program (2150526). We also thank Dr. Andrew G. Roberts for helpful discussions regarding the synthesis of the isotopologues and isotopomers.

For TOC Use Only:



References

- (1) Gabelica, V.; Marklund, E. Fundamentals of ion mobility spectrometry. *Curr. Opin. Chem. Biol.* **2018**, *42*, 51-59.
- (2) Dodds, J. N.; Baker, E. S. Ion Mobility Spectrometry: Fundamental Concepts, Instrumentation, Applications, and the Road Ahead. *J. Am. Soc. Mass Spectrom.* **2019**, *30* (11), 2185-2195.
- (3) Giles, K.; Ujma, J.; Wildgoose, J.; Pringle, S.; Richardson, K.; Langridge, D.; Green, M. A Cyclic Ion Mobility-Mass Spectrometry System. *Anal. Chem.* **2019**, *91* (13), 8564-8573.
- (4) Deng, L.; Ibrahim, Y. M.; Baker, E. S.; Aly, N. A.; Hamid, A. M.; Zhang, X.; Zheng, X.; Garimella, S. V. B.; Webb, I. K.; Prost, S. A.; et al. Ion Mobility Separations of Isomers based upon Long Path Length Structures for Lossless Ion Manipulations Combined with Mass Spectrometry. *ChemistrySelect* **2016**, *1* (10), 2396-2399.
- (5) Hollerbach, A. L.; Li, A.; Prabhakaran, A.; Nagy, G.; Harrilal, C. P.; Conant, C. R.; Norheim, R. V.; Schimelfenig, C. E.; Anderson, G. A.; Garimella, S. V. B.; et al. Ultra-High-Resolution Ion Mobility Separations Over Extended Path Lengths and Mobility Ranges Achieved using a Multilevel Structures for Lossless Ion Manipulations Module. *Anal. Chem.* **2020**, *92* (11), 7972-7979
- (6) Kirk, A. T.; Bohnhorst, A.; Raddatz, C.-R.; Allers, M.; Zimmermann, S. Ultra-high-resolution ion mobility spectrometry—current instrumentation, limitations, and future developments. *Anal. Bioanal. Chem.* **2019**, *411*, 6229-6246.
- (7) Hollerbach, A. L.; Li, A.; Prabhakaran, A.; Nagy, G.; Harrilal, C. P.; Conant, C. R.; Norheim, R. V.; Schimelfenig, C. E.; Anderson, G. A.; Garimella, S. V. Ultra-high-resolution ion mobility separations over extended path lengths and mobility ranges achieved using a multilevel structures for lossless ion manipulations module. *Anal. Chem.* **2020**, *92* (11), 7972-7979.
- (8) Paglia, G.; Smith, A. J.; Astarita, G. Ion mobility mass spectrometry in the omics era: Challenges and opportunities for metabolomics and lipidomics. *Mass Spectrom. Rev.* **2021**, *41* (5), 722-765.
- (9) Williamson, D. L.; Bergman, A. E.; Nagy, G. Investigating the Structure of α/β Carbohydrate Linkage Isomers as a Function of Group I Metal Adduction and Degree of Polymerization as Revealed by Cyclic Ion Mobility Separations. *J. Am. Soc. Mass Spectrom.* **2021**, 32 (10), 2573-2582.
- (10) Garimella, V. B. S.; Nagy, G.; Ibrahim, Y. M.; Smith, R. D. Opening new paths for biological applications of ion mobility Mass spectrometry using structures for lossless ion manipulations. *TrAC. Trends Anal. Chem.* **2019**, *116*, 300-307.
- (11) Nagy, G.; Attah, I.; Garimella, S.; Tang, K.; Ibrahim, Y.; Baker, E.; Smith, R. Unraveling the Isomeric Heterogeneity of Glycans: Ion Mobility Separations in Structures for Lossless Ion Manipulations. *Chem. Commun.* **2018**, *54*, 11701-11704.
- (12) Warnke, S.; Ben Faleh, A.; Scutelnic, V.; Rizzo, T. R. Separation and Identification of Glycan Anomers Using Ultrahigh-Resolution Ion-Mobility Spectrometry and Cryogenic Ion Spectroscopy. *J. Am. Soc. Mass Spectrom.* **2019**, *30* (11), 2204-2211.
- (13) Peterson, T. L.; Nagy, G. Toward Sequencing the Human Milk Glycome: High-Resolution Cyclic Ion Mobility Separations of Core Human Milk Oligosaccharide Building Blocks. *Anal. Chem.* **2021**, 93 (27), 9397-9407.
- (14) Williamson, D. L.; Bergman, A. E.; Heider, E. C.; Nagy, G. Experimental measurements of relative mobility shifts resulting from isotopic substitutions with high-resolution cyclic ion mobility separations. *Anal. Chem.* **2022**, *94* (6), 2988-2995.
- (15) Kirk, A. T.; Raddatz, C.-R.; Zimmermann, S. Separation of isotopologues in ultra-high-resolution ion mobility spectrometry. *Anal. Chem.* **2017**, *89* (3), 1509-1515.
- (16) Kaszycki, J. L.; Bowman, A. P.; Shvartsburg, A. A. Ion mobility separation of peptide isotopomers. *J. Am. Soc. Mass Spectrom.* **2016**, *27* (5), 795-799.

- (17) Wojcik, R.; Nagy, G.; Attah, I. K.; Webb, I. K.; Garimella, S. V.; Weitz, K. K.; Hollerbach, A.; Monroe, M. E.; Ligare, M. R.; Nielson, F. F. SLIM ultrahigh resolution ion mobility spectrometry separations of isotopologues and isotopomers reveal mobility shifts due to mass distribution changes. *Anal. Chem.* **2019**, *91* (18), 11952-11962.
- (18) Pathak, P.; Shvartsburg, A. A. High-Definition Ion Mobility/Mass Spectrometry with Structural Isotopic Shifts for Nominally Isobaric Isotopologues. *J. Phys. Chem. A* **2023**, *127* (17), 3914-3923. DOI: 10.1021/acs.jpca.3c01792.
- (19) Pathak, P.; Shvartsburg, A. A. High-Definition Differential Ion Mobility Spectrometry with Structural Isotopic Shifts for Anionic Compounds. *J. Am. Soc. Mass Spectrom.* **2023**, *34* (7), 1519-1523. DOI: 10.1021/jasms.3c00190.
- (20) Pathak, P.; Sarycheva, A.; Baird, M. A.; Shvartsburg, A. A. Delineation of Isomers by the 13C Shifts in Ion Mobility Spectra. *J. Am. Soc. Mass Spectrom.* **2021**, *32* (1), 340-345. DOI: 10.1021/jasms.0c00350.
- (21) Pathak, P.; Baird, M. A.; Shvartsburg, A. A. Structurally Informative Isotopic Shifts in Ion Mobility Spectra for Heavier Species. *J. Am. Soc. Mass Spectrom.* **2020**, *31* (1), 137-145. DOI: 10.1021/jasms.9b00018.
- (22) Baird, M. A.; Pathak, P.; Shvartsburg, A. A. Elemental Dependence of Structurally Specific Isotopic Shifts in High-Field Ion Mobility Spectra. *Anal. Chem.* **2019**, *91* (5), 3687-3693. DOI: 10.1021/acs.analchem.8b05801.
- (23) Pathak, P.; Baird, M. A.; Shvartsburg, A. A. Identification of Isomers by Multidimensional Isotopic Shifts in High-Field Ion Mobility Spectra. *Anal. Chem.* **2018**, *90* (15), 9410-9417. DOI: 10.1021/acs.analchem.8b02057.
- (24) Kaszycki, J. L.; Baird, M. A.; Shvartsburg, A. A. Molecular Structure Characterization by Isotopic Splitting in Nonlinear Ion Mobility Spectra. *Anal. Chem.* **2018**, *90* (1), 669-673. DOI: 10.1021/acs.analchem.7b04610 (accessed 2021-07-08T19:28:38).
- (25) Williamson, D. L.; Nagy, G. Isomer and Conformer-Specific Mass Distribution-Based Isotopic Shifts in High-Resolution Cyclic Ion Mobility Separations. *Anal. Chem.* **2022**, *94* (37), 12890-12898.
- (26) Williamson, D. L.; Trimble, T. K.; Nagy, G. Hydrogen-Deuterium-Exchange-Based Mass Distribution Shifts in High-Resolution Cyclic Ion Mobility Separations. *J. Am. Soc. Mass Spectrom.* **2023**, *34* (6), 1024-1034.
- (27) Williamson, D. L.; Nagy, G. Coupling Isotopic Shifts with Collision Cross-Section Measurements for Carbohydrate Characterization in High-Resolution Ion Mobility Separations. *Anal. Chem.* **2023**, *95* (37), 13992-14000.
- (28) Harrilal, C. P.; Gandhi, V. D.; Nagy, G.; Chen, X.; Buchanan, M. G.; Wojcik, R.; Conant, C. R.; Donor, M. T.; Ibrahim, Y. M.; Garimella, S. V. B.; et al. Measurement and Theory of Gas-Phase Ion Mobility Shifts Resulting from Isotopomer Mass Distribution Changes. *Anal. Chem.* **2021**, 93 (45), 14966-14975.
- (29) Harrilal, C. P.; Garimella, S. V.; Chun, J.; Devanathan, N.; Zheng, X.; Ibrahim, Y. M.; Larriba-Andaluz, C.; Schenter, G.; Smith, R. D. The Role of Ion Rotation in Ion Mobility: Ultrahigh-Precision Prediction of Ion Mobility Dependence on Ion Mass Distribution and Translational to Rotational Energy Transfer. *J. Phys. Chem. A* **2023**.
- (30) Ujma, J.; Ropartz, D.; Giles, K.; Richardson, K.; Langridge, D.; Wildgoose, J.; Green, M.; Pringle, S. Cyclic Ion Mobility Mass Spectrometry Distinguishes Anomers and Open-Ring Forms of Pentasaccharides. *J. Am. Soc. Mass Spectrom.* **2019**, *30* (6), 1028-1037.
- (31) Sommer, H. Z.; Jackson, L. L. Alkylation of amines. New method for the synthesis of quaternary ammonium compounds from primary and secondary amines. *J. Org. Chem.* **1970**, 35 (5), 1558-1562.
- (32) Vollhardt, K. P. C.; Schore, N. E. *Organic chemistry: structure and function*; Macmillan, 2003.

- (33) Habibi, S. C.; Nagy, G. General Method to Obtain Collision Cross-Section Values in Multipass High-Resolution Cyclic Ion Mobility Separations. *Anal. Chem.* **2023**.
- (34) Breen, J.; Hashemihedeshi, M.; Amiri, R.; Dorman, F. L.; Jobst, K. J. Unwrapping Wraparound in gas (or Liquid) Chromatographic Cyclic Ion Mobility–Mass Spectrometry. *Anal. Chem.* **2022**, *94* (32), 11113-11117.
- (35) D'Atri, V.; Porrini, M.; Rosu, F.; Gabelica, V. Linking molecular models with ion mobility experiments. Illustration with a rigid nucleic acid structure. *Journal of Mass Spectrometry* **2015**, *50* (5), 711-726.
- (36) Frisch, M.; Trucks, G.; Schlegel, H. B.; Scuseria, G.; Robb, M.; Cheeseman, J.; Scalmani, G.; Barone, V.; Petersson, G.; Nakatsuji, H. Gaussian 16. Gaussian, Inc. Wallingford, CT: 2016.
- (37) Damas, G. B.; Dias, A. B.; Costa, L. T. A quantum chemistry study for ionic liquids applied to gas capture and separation. *J. Phys. Chem. B* **2014**, *118* (30), 9046-9064.
- (38) Ochterski, J. W. Vibrational analysis in Gaussian. 1999. https://gaussian.com/vib/ (accessed 2024 January 22nd).